Chemosphere 269 (2021) 129327

Contents lists available at ScienceDirect

Chemosphere

journal homepage: www.elsevier.com/locate/chemosphere

Accountancy for intrinsic colloids on thorium solubility: The fractionation of soluble species and the characterization of solubility limiting phase

Rama Mohana Rao Dumpala [a, b, *], Manjulata Sahu [b, c], Brijlesh K. Nagar [c], Vaibhavi V. Raut [c], Naina H. Raje [d], Neetika Rawat [a], Jeyakumar Subbiah [c], Manoj Kumar Saxena [c], Bhupendra S. Tomar [b]

[a] Radiochemistry Division, Bhabha Atomic Research Centre, Mumbai, 400085, India
[b] Homi Bhabha National Institute, Training School Complex, Anushaktinagar, Mumbai, 400094, India
[c] Radioanalytical Chemistry Division, Bhabha Atomic Research Centre, Mumbai, 400085, India
[d] Analytical Chemistry Division, Bhabha Atomic Research Centre, Mumbai, 400085, India

HIGHLIGHTS

- The experimental conditions plays crucial role on colloid size and concentrations.
- Present methodology allows detection of colloids of lower size at low concentrations.
- The soluble thorium was fractionated to ionic, polymeric, and colloidal forms.
- The exclusion of colloids overestimates the solubility limits 2–4 orders.
- The precipitate formed is amorphous in nature and are micro crystalline.

GRAPHICAL ABSTRACT

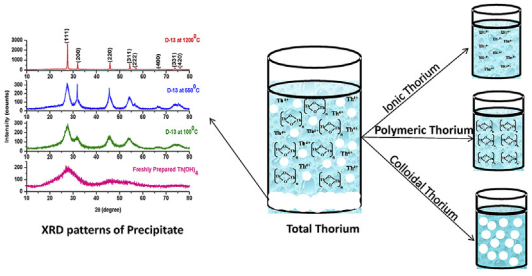

ARTICLE INFO

Article history:
Received 24 June 2020
Received in revised form
10 December 2020
Accepted 13 December 2020
Available online 24 December 2020

Handling Editor: Martine Leermakers

Keywords:
Thorium colloids
Laser induced breakdown detection (LIBD)
Aqueous speciation
Fractionation
Solubility
Solubility product

ABSTRACT

The extensive hydrolysis of tetravalent actinides leads to polynuclear formations through oxygen bridging facilitating the formation of colloids as end products. The pH, ionic strength has phenomenal effects on Thorium colloids formation. The quantitative estimation of colloids facilitates the fraction of soluble fraction into ionic, polymeric and colloidal forms of thorium. The colloids accountability and precipitate characterization explains the discrepancies in estimated solubility limits. The supernatants of long equilibrated (~3 years) saturated thorium solution under various pH (5- 11) and ionic strengths (0 −3 M $NaClO_4$) were analysed by Inductively Coupled Plasma Mass Spectrometer (ICP-MS) and Ion Chromatography (IC) to determine total and ionic thorium respectively. Laser Induced Breakdown Detection (LIBD) was employed to determine the colloid size and concentrations. The precipitates were characterized by calorimetry and XRD to determine the solubility limiting phase. The results of pH, IC, ICP-MS, and LIBD measurements on the aged thorium samples are discussed with regard to the mechanism of the formation of thorium colloids. The results revealed the formation of colloids having particle size (10–40 nm) at concentrations (10^9-10^{11} particles/mL). The colloids accountancy resulted in estimated solubility products to 2–4 orders lower than their inclusion as soluble thorium. The soluble

* Corresponding author. Radiochemistry Division, Bhabha Atomic Research Centre, Mumbai, 400085, India.
E-mail address: rammohan@barc.gov.in (R.M.R. Dumpala).

https://doi.org/10.1016/j.chemosphere.2020.129327
0045-6535/© 2020 Elsevier Ltd. All rights reserved.

thorium was fractionated quantitatively into ionic, polymeric and colloidal forms of thorium. The precipitates formed are found to be semi amorphous.

© 2020 Elsevier Ltd. All rights reserved.

Credit author statement

Rama Mohana Rao Dumpala: Conceptualization, Methodology, Validation, Formal analysis, Investigation, Resources, Data curation, Writing – original draft, Writing – review & editing, Supervision, Manjulata Sahu: Investigation –TG-DSC, Formal analysis, Writing – original draft, Writing – review & editing; Brijlesh K Nagar: Investigation –ICP-MS; Vaibhavi V Raut: Investigation - IC; Naina H Raje: Investigation; Neetika Rawat: Supervision; Jeyakumar Subbiah: Supervision; Manoj K Saxena: Supervision; Bhupendra S Tomar: Writing – review & editing, Supervision.

1. Introduction

The nuclear power production and the various nuclear fuel processing activities from mining to reprocessing, transportation to storage of radioactive waste and finally the disposal of high level waste can cause accidental release of actinides to the environment (Allard et al., 1984). The studies on transportation and migration behaviour of actinides in natural and engineered barriers is a key input for the safe and secure storage and monitoring of nuclear waste repositories including the world-wide proposed deep geological repositories (Natrajan et al., 2014). The actinides in aquatic environment can undergo precipitation, sorption, and complexation or colloid formation depending on the surrounding geochemical conditions (Silva and Nitsche, 1995). The actinide as ionic, polymeric and as colloid will show different chemical properties which in turn would impact the migration patterns of the same. The colloids, being able to suspend in the aqueous phase will always contribute to the higher levels of radioactivity in transportation and migration phenomenon (Honeyman, 1999; Kalmykov and Denecke, 2011; Walther and Denecke, 2013). Thus, the colloid contribution is a crucial factor to estimate solubility limits accurately which are prerequisites for a reliable geochemical modelling of the waste confinements.

The actinide ions in aquatic environment forms two different kinds of colloids: The real or Eigen colloids, which are formed by actinide hydrolysis leading to subsequent formation of polymeric species and finally transform to colloids; pseudo colloids, formed by actinide ions sorption on to either the real colloids or the aquatic colloids already present in water (Kim et al., 1987). Actinide ions with higher oxidations state, particularly tetravalent ions undergo hydrolysis, which eventually leads to formation of polymeric species via, -oxo- bridging and ultimately transform into colloids. The size, composition, and structure of actinide real colloids depend on mode of formation, their source, and history (Kalmykov and Denecke, 2011). Depending on the size and surface charge present, the actinide colloids can enhance or retard the migration of actinides in the aquatic environments (Honeyman, 1999). Thus, it is essential to take into account the intrinsic colloids for accurate prediction of the migration rates of actinides in geosphere (Bates et al., 1992). The literature on the source, formation and interaction of colloids as well as their role in the migration of actinides has been reviewed by Walther and Denecke (2013) recently. The literature reported solubility data show considerable discrepancies (log K_{SP} varies from −45.5 to −54.2) for amorphous Th(IV) precipitates (Ryan and Rai, 1987; Rai et al., 2000; Jernstrom et al., 2001; Neck and Kim, 2001; Rothe et al., 2002; Neck et al., 2003; Xia et al., 2003; Altmaier et al., 2005).

The actinide colloids in aquatic media are often detected by absorption spectroscopy, light scattering methods, and by laser-induced breakdown detection (LIBD) (Walther, 2003; Walther and Denecke, 2013). The Laser-Induced Breakdown Detection (LIBD) is a highly sensitive technique for the quantification of aquatic colloids of smaller size (<50 nm) in very low concentrations (ppb to ppt), which cannot be detected by conventional light scattering methods (Kim and Walther, 2006). LIBD technique was extensively used for characterization of actinide colloids to understand their genesis, formation, to estimate solubility, and migration effects under various geochemical environments (Kim and Walther, 2006; Bitea et al., 2003; Neck et al., 2002; Bundschuh et al., 2000). But, to best of our knowledge no reports are available on studies on the colloid of Th(IV) in aqueous perchlorate media over a range of ionic strength and hydrogen ion concentration kept for a long period of equilibration (~3 years). Further, though the thorium colloids genesis and characterization was reported in the literature, there were no studies on concentrations of colloids present as well as fractionation of soluble content to different form of species, such as, ionic, polymeric and colloids. Thus, the studies on factors influencing the formation and characterization of actinide intrinsic colloids are essential to estimate the true solubility of the actinides and hence the colloid contributions to the actinide speciation. Further, the true nature of intrinsic colloid formation could be revealed by usage of a proper background electrolyte. The poor nucleophiliicity, non-coordinating nature, and inertness to redox processes make the perchlorate anion as a best electrolyte to carry out the metal ion interaction and speciation studies (Brown and Gu 2006). Thus, the present studies also carried out in aqueous perchlorate medium. The present studies aimed at (i) To interpret the mechanism of colloid formation; (ii) The effect of centrifugation speed on colloid aggregation; (iii) Size and concentration distribution of intrinsic colloids; (iv) Determining the pH effect on colloid contribution; (v) Revealing the role of ionic strength on colloid as well as precipitate formation; (vi) Fractionation of soluble thorium species into ionic, polymeric and colloidal forms; (vii) Solubility estimation by accounting the colloid contribution; (viii) identifying the solubility limiting phases; The pH measurements, characterization of colloids for their size and concentrations, measurement of ionic thorium, characterization of thorium precipitate formed at higher pH and ionic strength are carried out to achieve the above mentioned targets of the study.

2. Material and methods

All the materials used were of analytical grade and above and complete details on purity and preparation were given in supporting information (SI). All the samples were prepared in 30 mL Oak Ridge centrifuge tubes. Oversaturation method was employed for the sample preparations in which excess of thorium perchlorate solution was equilibrated with the solution of desired pH and ionic strength. Each tube contains 10 mL of 0.01 M (2320 μg/mL) thorium solution under various pH (5–11) and ionic strength (0–3 M $NaClO_4$). All the samples were prepared under an inert atmosphere provided by continuous purging nitrogen at 298 K. All the samples

kept at various ionic strengths were designated with alphabets (A-D) for ease in data interpretation (sample code details are given in Table S1 of SI).

The adjustment and measurement of pH was done by an auto-titrator Metrohm (Model no. 716 DMS Titrino). The preparation and calibration of electrode was provided elsewhere (Rao et al., 2013). The Dionex ion chromatographic system and a VG Plasma Quad PQ II (V. G. Elemental, Winsford, Cheshire, England) ICP-MS were used for the determination of ionic and total thorium in supernatants respectively. LIBD system called MAGELLAN developed by Cordouan Technologies (France) in collaboration with the Karlsruhe Institute of Technology (KIT), Germany was used for determination of size and concentration of thorium colloids formed. High Temperature Thermo Gravimetric Differential Thermal Analyses (HT-TG-DSC) in combination with X-ray diffraction (XRD) studies were carried out to characterize the precipitate formed by the aged thorium perchlorate solutions. All the details of the techniques employed in the present studies were given in supporting information (S1).

3. Results and discussions

The long equilibrated thorium samples are initially tested to optimize the centrifugation parameters. Then, the supernatant was separated to analyse the thorium present as dissolved thorium species. The supernatant solutions were subjected to pH, IC and ICP-MS measurements to characterize the aqueous soluble species, LIBD analysis to account the colloid contribution; while the precipitates were subjected to HT-TG-DSC and XRD measurements to determine the solubility limiting phase.

3.1. Mechanism of colloid formation

The extensive hydrolysis of actinides facilitates the polynuclear species formation through either, olation where hydroxyl bridges are formed, or oxolation where oxo bridges are formed (Henry et al., 1992). The olation path is the more dominant one for highly charged actinide ions (Choppin and Jensen, 2010). The initially formed hydroxo-bridged thorium polynuclear hydroxides would facilitate the formation of either mono oxygen bridged thorium polynuclear species (Scheme X in Fig. 1) or double oxygen bridged thorium polynuclear structures (Scheme Y in Fig. 1). Scheme X proceeds through eviction of a water molecule, while Scheme Y proceeds through eviction of two protons to form the polymeric species. This would subsequently result in the formation of colloids or precipitate formation depending on the initial conditions of equilibration like pH and ionic strength. Scheme X results in no change in H^+ concentration after equilibration periods, while Scheme Y result in increasing the hydrogen ion concentration (or decreasing the pH) at the end of equilibration period.

The pH measured for the samples kept at various initial pH and ionic strengths after an equilibration period of ~3 years are given in Table 1. Except, for samples kept at I = 1 M and 3 M $NaClO_4$ at an initial pH of 13 and for the sample at I = 3.0 M $NaClO_4$ and initial pH at 11, all other samples were found to drop down the pH to lower values after equilibration period. This is attributed to the release of H^+ ion, hence the lowering in pH values after equilibration. This can be possible only when thorium forms polynuclear chains by double oxo-bridging resulting in colloids formation by release of H^+ ions. Further, the samples kept at high ionic strength have larger drop in pH values than the sample kept at lower ionic strengths. The samples initially kept at pH 11 except the sample at I = 3.0 M $NaClO_4$ (No change in pH) showed more change in pH after equilibration. The samples kept at an initial pH of 13 at all ionic strengths and for the sample at I = 3.0 M $NaClO_4$ and initial pH at 11 showed no change or minimal change in pH after equilibration. This smaller or no variation in pH after equilibration period could be attributed to the strong tendency for precipitate formation under these experimental conditions at the very beginning of the equilibration period.

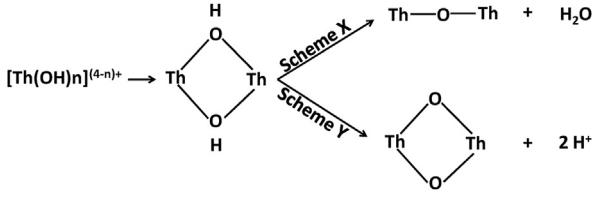

Fig. 1. One-dimensional simplified schematic representation for the polynucleation mechanism of the thorium hydroxides in aqueous solutions.

Table 1
Measured pH values of different thorium perchlorate samples after an equilibration period of ~1080 days at T = 298.15 K and P = 0.1 M Pa.

Initial pH → Ionic Strength ↓	5.00	7.00	9.00	11.00	13.00
0.0 M $NaClO_4$	2.89	2.98	3.30	6.18	12.17
0.1 M $NaClO_4$	2.88	3.04	3.33	6.84	12.46
1.0 M $NaClO_4$	2.86	2.89	3.66	8.48	13.00
3.0 M $NaClO_4$	2.69	2.85	3.09	11.00	13.00

*Standard uncertainties u are u(T) = 0.1 K, u(p) = 10 k Pa, and u(pH) = 0.01. (Level of confidence = 0.95).

3.2. The effect of centrifugation speed on colloid aggregation

The time and rate of centrifugation plays a key role in settling the particles down to form the precipitates. Thus, before characterizing the colloid particles for the size and concentration determination, few samples were centrifuged for different time periods at different centrifugation rates for 60 min. The samples are centrifuged at 0, 3000, 9000, 15000 and 16,500 rpm (Fig. 3A). The samples showed no change in characteristic LIBD patterns with increase in centrifugation rate beyond 16,500 rpm. Then the centrifugation time was varied for 15, 30, 45 and 60 min, but the samples showed no variation in LIBD patterns with time. Thus, all the samples for further analysis are centrifuged at 16,500 rpm for 30 min as the optimum conditions to avoid the suspension of larger particles in the supernatants of the samples. To ascertain that there is no interference of either the background electrolyte ($NaClO_4$) or the Milli-Q water on sample characterization, initially the LIBD measurements were carried for two thorium samples at pH 5 and 7, ultrapure water, 0.1 M and 1.0 M $NaClO_4$ (Fig. 3B). Thus, the samples breakdown happens well before the breakdown of background electrolyte ($NaClO_4$) and the medium (water).

3.3. Identification of colloids: quantification by size and concentration

The equilibrated thorium samples were initially centrifuged at 16,500 rpm for 30 min and the supernatants were collected for colloid characterization. Prior to LIBD analysis, all the supernatants were passed through 0.1 μm membrane filter to avoid the larger particles. The size and concentration of the colloid particles was measured by LIBD technique. The LIBD plots (variation of BDP with laser energy) for all the Thorium samples at constant pH and ionic strength are shown in Fig. 2C and D respectively. Similar LIBD plots for all other samples were also recorded to find out the threshold

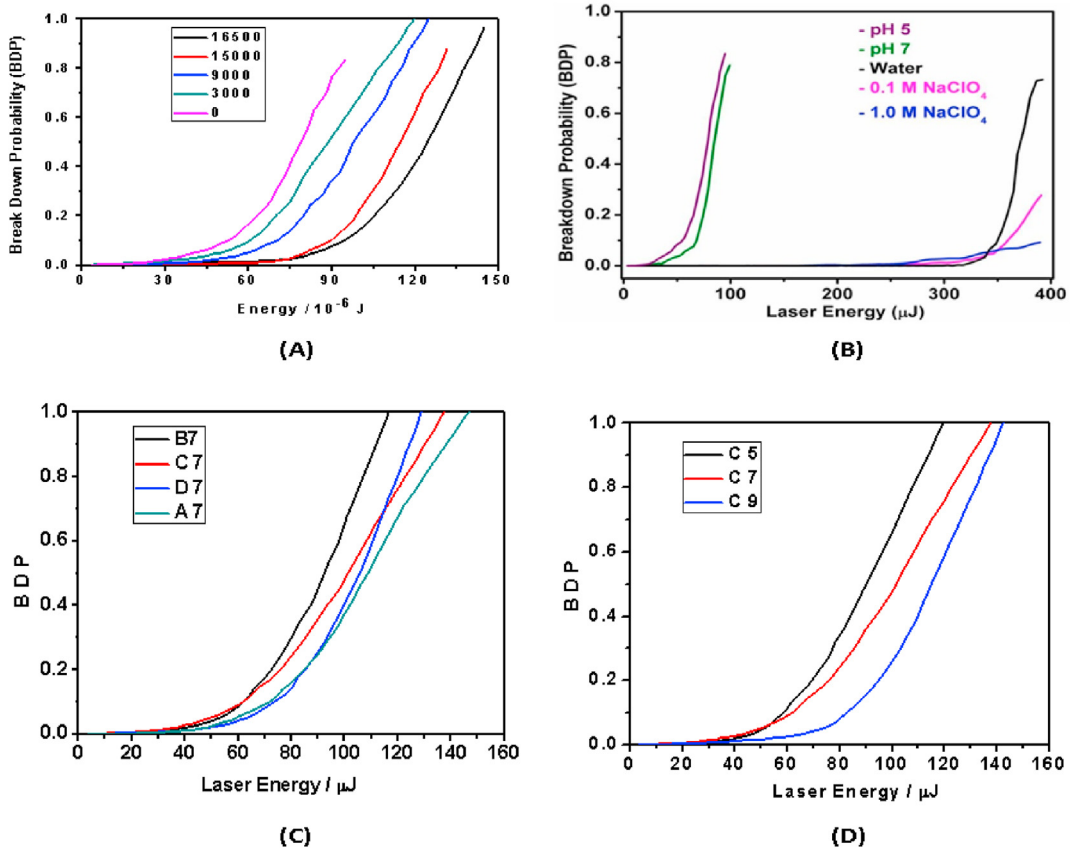

Fig. 2. (A). The effect of centrifugation rates on colloid settling and its characterization. **(B).** The LIBD patterns (plots of breakdown probability (BDP) Vs. Laser Energy) for ultrapure water, 0.1 M and 1.0 M $NaClO_4$ along with the real samples of thorium which were kept at an initial pH of 5 and 7. **(C).** The breakdown probabilities of thorium colloids formed in the thorium perchlorate samples kept at constant initial pH (=7) and at various ionic strengths for an equilibration of 3 years. **(D).** The breakdown probabilities of thorium colloids formed in the thorium perchlorate samples kept at constant ionic strength (= 1.0 M $NaClO_4$) but at various initial pH for an equilibration of 3 years.

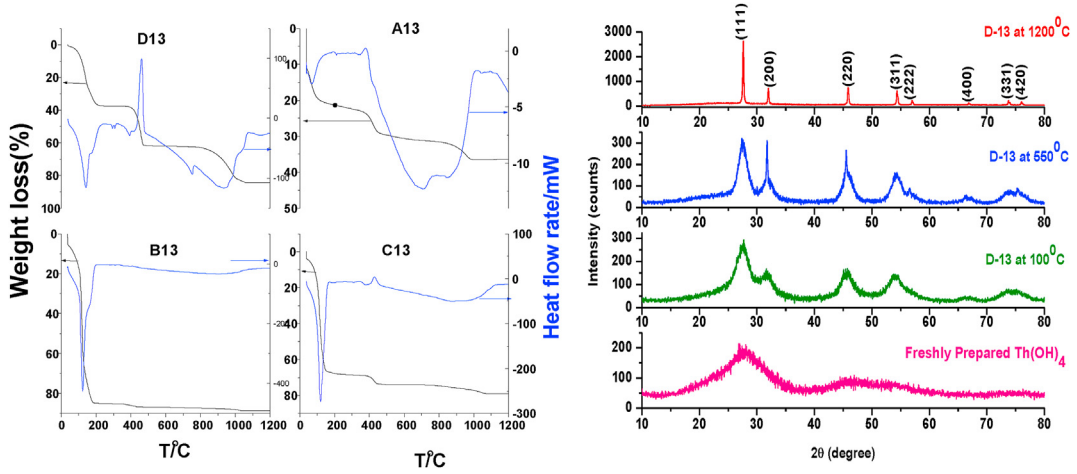

Fig. 3. (A). TG-DSC pattern of precipitates resulted from the equilibrated samples at pH = 13 under different ionic strengths (A13, B13, C13 and D13 samples). (Black: Weigh loss and Blue: Heat flow). **(B).** XRD patterns of the residues obtained at the end of each peak in thermogram for the aged thorium sample (D-13) along with a freshly prepared $Th(OH)_4$. (For interpretation of the references to color in this figure legend, the reader is referred to the Web version of this article.)

energy and slope of the LIBD patterns. The LIBD patterns were found to be very close to each other with respect to breakdown probability and slope. This behaviour signified narrow variations in sizes and concentrations of the colloids formed in all the samples. The threshold values (the point of BDP = 0.01) for all the samples were found to spread over a range of 25–40 μJ which corresponds to a particle diameter in the range of 10–40 nm. The quantification of colloids by size (diameter) and concentrations (particles/mL) determined by LIBD are shown in Table 2. The table shows that the colloids as small as 13 nm and as low as 10^{10} particles/mL can be quantified by using LIBD technique.

Table 2
Size (diameter) and concentration (particles/mL) of the thorium colloids under various initial pH and ionic strength conditions; and the fractionation of total thorium content present in the supernatants as ionic, colloidal, and polymeric form of thorium (in M).

Ionic Strength	Initial pH	Sample	Size/nm	$Th_{Colloid}/10^{10}$ particles/mL)	$Th_{Total}/10^{-10}$ M)	$Th_{Ionic}/10^{-10}$ M)	$Th_{Colloid}/10^{-10}$ M)	$Th_{Polymeric}/10^{-10}$ M))
0.0 M $NaClO_4$	5.00	A5	19.6 ± 1.6	57.69	9.67	2.96	5.06	1.65
	7.00	A7	13.6 ± 1.8	62.01	5.72	1.64	1.81	2.27
	9.00	A9	13.4 ± 1.8	26.40	3.90	1.12	0.75	2.03
	11.00	A11	BDL	BDL	0.09	0.06	BDL	0.02
	13.00	A13	BDL	BDL	0.04	0.01	BDL	0.03
0.1 M $NaClO_4$	5.00	B5	20.6 ± 2.2	47.17	9.062	2.43	4.83	1.80
	7.00	B7	27.9 ± 2.0	04.42	3.47	0.36	1.13	1.98
	9.00	B9	34.3 ± 1.8	02.20	1.95	0.13	1.04	0.78
	11.00	B11	BDL	BDL	0.05	BDL	BDL	0.05
	13.00	B13	BDL	BDL	0.01	BDL	BDL	0.01
1.0 M $NaClO_4$	5.00	C5	22.5 ± 2.1	32.40	7.28	2.10	4.31	0.88
	7.00	C7	34.7 ± 1.7	02.22	2.56	0.90	1.06	0.61
	9.00	C9	14.2 ± 2.5	29.86	1.35	BDL	1.00	0.35
	11.00	C11	BDL	BDL	BDL	BDL	BDL	BDL
	13.00	C13	BDL	BDL	BDL	BDL	BDL	BDL
3.0 M $NaClO_4$	5.00	D5	17.3 ± 2.5	46.03	4.83	0.85	2.80	1.18
	7.00	D7	13.1 ± 2.4	33.72	1.37	0.30	0.88	0.19
	9.00	D9	26.0 ± 2.0	03.22	0.78	BDL	0.66	0.11
	11.00	D11	BDL	BDL	BDL	BDL	BDL	BDL
	13.00	D13	BDL	BDL	BDL	BDL	BDL	BDL

*BDL - Below Detection Limits; Standard uncertainties u are u(T) = 0.1 K, u(p) = 10 k Pa, and the combined expanded uncertainties Uc (size) for each set of data was given in the table, the combined expanded uncertainties Uc (concentration given as particles/mL) are $\leq 0.01 \times 10^{10}$ particles/mL and, the combined expanded uncertainties Uc (concentration given as M) are $\leq 0.01 \times 10^{-10}$ M. (Level of confidence = 0.95). The detection limits for IC, ICP-MS and LIBD are 1 ng/mL (4.3E-12 M), 0.1 ng/mL (4.3E-13 M), and 10^8 particles/mL respectively.

3.4. Effect of pH and ionic strength on colloid formation

The pH and ionic strength play a key role in deciding the speciation of thorium hydrolysis. Thus, the construction of speciation plots would be very informative to know the exact species present at a particular combination of pH and ionic strength. The speciation plots for hydrolysis of thorium at various ionic strengths are constructed from the known hydrolysis constants (Figure S2 in SI). The polynuclear hydrolytic species are the precursors for colloid formation. The formation of $[Th_6(OH)_{15}]^{9+}$ is the major contributor in the pH range 4–10, while above pH 10, the formation of $[Th(OH)_4]$ escalates as an end product. Thus, there was no colloid formation observed at pH $\geq$ 11 at all ionic strength due to high probability of precipitate formation (as $[Th(OH)_4]$) than colloid aggregation. In addition, there could be either very small size (<1 nm) and/or at very low concentration of aggregate formation ($<10^8$ - particles/mL) which could not be detected by the present instrumental parameters. Thus, at the pH $\geq$ 11, the LIBD analysis showed both the size and concentrations to be below detection limits. For a particular ionic strength, the concentration of colloid particles decreases with increase in initial pH except at I = 1.0 M $NaClO_4$. This is attributed to the increased tendency to form precipitates at higher pH. At acidic initial pH (=5), the colloid concentrations follow an ascending trend with ionic strength. While a dip in colloid concentrations at I = 0.1 M $NaClO_4$ is observed with ionic strength at higher pH (= 7 or 9) conditions. There is a cumulative influence of both the ionic strength and pH on colloid formation at higher pH.

3.5. Fractionation of soluble thorium species

The soluble thorium in supernatant can be either Th^{4+} aqua ion or as monomeric/polymeric thorium hydroxide species or as dissolved Eigen colloids. The present studies made an attempt to categorize the soluble species into the three categories as ionic, polymeric, and colloidal forms. The ion chromatography (IC) technique was used to identify the concentration of ionic thorium (designated as Th_{Ionic} in Table 2) as Th^{4+} ion. The retention time and peak area of a standard thorium solutions was employed for the identification and quantification of Th^{4+} ion respectively. ICP-MS technique was used for the determination of total Thorium concentration in the supernatant. The aliquots of supernatant solutions are diluted with 1% conc. HNO_3 to determine the total thorium content (designated as Th_{Total} in Table 2) in supernatant by ICP-MS. The difference in concentration determined by ICP-MS to IC gives the amount of thorium present in non-ionic form (other than Th^{4+}) either as polymeric or colloidal forms. Walther et al. (2008) used electro-spray ionization mass-spectrometry (ESI-MS), to determine the contribution of various mononuclear, dimeric and polynuclear thorium hydroxide species present in various solutions of thorium (6×10^{-6} to 10^{-1} M in the pH range of 1–4) kept for equilibration for a time period of one week to 48 days. They found the presence of a large number of polynuclear species and extent of polynucleation was found to increase with pH. In the present study the samples were kept for equilibration at higher pH and for longer time duration (~3 years). Thus, the polynuclear species would likely to dominate under the present conditions, which subsequently converted to colloids. So, the difference in concentration of thorium determined by ICP-MS and IC can be attributed to the presence of polynuclear species and detectable colloid particles. Hence, if the concentration of the colloid particles can be found out, the content of thorium as polymeric species can be determined. For this, LIBD technique was employed to estimate the size and concentrations of the colloid particles.

The extensive hydrolysis of thorium facilitate the polynuclear formation and $Th_6(OH)_{15}^{9+}$ is a predominant polynuclear species (Figure S2) at total Th(IV) concentration (10^{-3} to 1 M) at pH 4.5–5.0 (Wickleder et al., 2010). Recently Knope et al. studied hexanuclear Th(IV)-hydrolysis species and found that the two nearest thorium neighbors are at 3.90–3.94 A^0 distance (Knope and Soderholm, 2013; Knope et al., 2011); and is in agreement with the Th–Th distance (3.94 A^0) in polynuclear species determined by Johansson (1968). Thus, in the present studies, total number of Th^{4+} ions present in each colloid was calculated by considering the Th–Th inter-atomic distance as 3.94 A^0 (Knope et al., 2011; Johansson, 1968). The total number of Th^{4+} ions present in each

colloid was multiplied with respective concentrations determined by LIBD (Table 2) to get the content of thorium present as colloidal form(designated as $Th_{Colloid}$ in Table 2). From the data on number of Th^{4+} ions as colloids, the total number of Th^{4+} ions as polymeric form can be calculated with the results obtained from IC and ICP-MS analysis of the samples. As IC, ICP-MS, LIBD gives thorium content present in the supernatants of the samples as Th^{4+} aqua ions, total thorium content and colloid contributions, respectively; the subtraction of concentration of thorium determine by IC and LIBD from the concentration determined by ICP-MS would give the thorium content, which is neither in colloidal nor in Th^{4+} aqua ion form. This amount of thorium, which excludes the colloid contribution, is present as soluble polymeric species in the supernatant and contributes to the solubility of thorium.

From Table 2, it is clear that both the total thorium, thorium as $Th^{4+}$and the contribution of colloids in supernatant follows a descending order with the increase in initial pH of the sample. This can be attributed to the enhancement in precipitation process as the initial pH of sample increases. The samples kept at 0.1 M ionic strength (B11 and B13) showed no thorium as Th^{4+} or as colloidal form and the very low amount of thorium detected (4.8×10^{-12} and 1.4×10^{-12} M respectively) is predominantly in the polymeric form. The overall thorium content present in supernatant of the samples kept at an initial pH of 11 and 13 at I = 1.0 and 3.0 M $NaClO_4$ was below detection limits for both the IC and ICP-MS analysis indicating a complete precipitation of the entire thorium.

3.6. Characterization of precipitate

The chemical form, the extent of hydrolysis, and the colloid contributions are the key factors behind the differences between reported solubility data up to 3–4 orders of magnitude for amorphous thorium oxyhydroxides. Hence the probable chemical composition of the precipitate was determined from the various thermal event appeared in thermogram obtained from TG-DSC run. Depending on the ageing periods, the precipitate could be completely amorphous ($Th(OH)_4$) or in a form ($ThO_2.2H_2O$) between the crystalline and amorphous nature. The amorphous $Th(OH)_4$ is known to be stable at 260–450 °C and gets transformed to ThO_2 at higher temperature (Wickleder et al., 2010). For, freshly prepared $Th(OH)_4$ (Figure S3 in SI), there are two weight loss events observed. The loss of occluded water occurred in the range 100° to 200 °C which was reflected with an endothermic peak in heat flow rate curve. At the end of temperature range ~200 °C, $Th(OH)_4$ formed and decomposed to ThO_2 around 300 °C which leads to a tail. The loss in weight is also calculated to be ~12% which is similar to the theoretical loss for the formation of oxide from $Th(OH)_4$. The exothermic peak in DSC around 295 °C, could be attributed to stronger bond formation in ThO_2 as compared to that of $Th(OH)_4$. Hence more energy would have been released in expense of breaking of hydroxide bonds of $Th(OH)_4$ and appeared as exothermic peak.

The thermogram of the thorium aged precipitates formed at all ionic strengths at initial pH of 13 (Fig. 3A) are found to be quite different from the thermogram of freshly prepared thorium precipitates (Figure S3). There were three weight loss processes observed whereas for freshly prepared hydroxide it was two step process, which signify presence of more than one species in the precipitate in addition to $Th(OH)_4$. The first sloping step till 200 °C is due to loss of occluded water, the corresponding % weight losses are not similar in the entire sample, which could be due to the precipitates taken directly without further processing. The second mass loss in the region ~370–400 °C represented by exothermic peak in heat flow curve could be explained similar to above, means the formation of $Th(OH)_4$ releases more heat than the heat required to break the bonds of its precursor species (polymeric species/colloids) initially would have present (product remained after heating at ~200 °C). The sample size of B13 was very small, which could be the reason for no visible exothermic peak. So polymeric species with weaker bond strength decomposed to ThO_2 and remaining part to $Th(OH)_4$ in the second step. The third mass loss at ~900 °C by the decomposition of $Th(OH)_4$ and remaining polynuclear species with stronger bond strength to form ThO_2. The third step in heat flow curve is a broad endothermic peak. The exact percentage loss, temperature of thermal event and the type of reaction (endo/exo) are given in Table 3. The thermograms inferred presence of more than one species in the aged precipitate which resulted in difficulty in assigning the mass losses to specific processes.

Table 3
The percentage of weight loss, temperature and the type of thermal event (endo/exo) of the precipitate obtained in equilibrated samples at pH = 13 under different ionic strengths (A13, B13, C13 and D13 samples).

Sample	T (in °C)	% Wt. loss	Type of thermal event
A13	100–150	20	Endo
	386.6	8.9	Exo
	901.0	5.1	Endo
B13	120	83	Endo
	371	1.9	not visible due to small sample size
	960	1.4	Endo
C13	98	67	Endo
	400.7	5.4	Exo
	899.5	4.9	Endo
D13	100–200	37	Endo
	425	24.7	Exo
	897.3	22.0	Endo

The residues obtained for sample D13 after each thermal event in TG-DSC was characterized by XRD and the respective diffractograms at 100 °C, 550 °C and 1200 °C are given in Fig. 3B. The diffractograms obtained for freshly prepared $Th(OH)_4$ was also included in Fig. 3B. The XRD of the precipitate formed in aged thorium solution (D13) at 100 °C was typical of an amorphous solid indicating that it is neither completely $Th(OH)_4$ nor ThO_2, can be called as amorphous hydrous oxyhydroxide $ThO_n(OH)_{4-2n}\cdot xH_2O$ (am) with $0 < n < 2$ and ThO_2 as the peaks correspond to the reported XRD peaks of ThO_2(ICSD Code 253564). The residue obtained at 550 °C also showed an identity of amorphous powder similar to the sample at 100 °C, but the sharp XRD peaks were originated indicating the formation of crystalline ThO_2 from amorphous precursor. The XRD pattern of residue obtained at 1200 °C corresponded to crystalline ThO_2. Thus the analysis with TG-DSC and XRD showed that the precipitate formed in aged Thorium solution was initially amorphous (hydrated thoria), which transformed to crystalline ThO_2 upon heating.

3.7. Solubility of thorium hydrous oxide [$Th(OH)_4$]

The solubility of either hydrous thorium oxyhydroxide ($ThO_2.2H_2O$) or the amorphous thorium hydroxide ($Th(OH)_4$) in aqueous solutions is generally given by the relation:

$$ThO_2.2H_2O\ (am,\ hydrous)\ or\ Th(OH)_4(am) \Leftrightarrow Th(OH)_4(aq) \quad (1)$$

$$Th(OH)_{4aq} \Leftrightarrow {Th^{4+}}_{aq} + 4\ {OH^-}_{aq} \quad (2)$$

And the solubility product (K_{SP}) is given by the relation

Table 4
The solubility and solubility products of thorium oxy(hydroxide) at different pH and ionic strengths at T = 298.15 K and P = 0.1 M Pa.

Ionic Strength	Initial pH	Sample Label	S (in 10^{-10}M) with Colloids	log K_{SP} with Colloids	S (in 10^{-10} M) w/o Colloids	log K_{SP} w/o Colloids
0.0 M $NaClO_4$	5.00	A5	9.668 ± 0.009	−42.66	4.611 ± 0.009	−44.27
	7.00	A7	5.724 ± 0.006	−43.80	3.912 ± 0.008	−44.63
	9.00	A9	3.905 ± 0.004	−44.63	3.158 ± 0.005	−45.09
0.1 M $NaClO_4$	5.00	B5	9.062 ± 0.009	−42.80	4.236 ± 0.009	−44.46
	7.00	B7	3.468 ± 0.003	−44.89	2.339 ± 0.003	−45.75
	9.00	B9	1.952 ± 0.002	−46.14	0.909 ± 0.005	−47.80
1.0 M $NaClO_4$	5.00	C5	7.284 ± 0.007	−43.28	2.978 ± 0.008	−45.22
	7.00	C7	2.564 ± 0.003	−45.55	1.508 ± 0.006	−46.70
	9.00	C9	1.355 ± 0.001	−46.93	0.353 ± 0.002	−49.85
3.0 M $NaClO_4$	5.00	D5	4.832 ± 0.005	−44.17	2.029 ± 0.006	−46.01
	7.00	D7	1.371 ± 0.001	−46.91	0.487 ± 0.002	−49.15
	9.00	D9	0.780 ± 0.001	−48.13	0.119 ± 0.009	−52.22

*w/o - without; Standard uncertainties u are u(T) = 0.1 K, u(p) = 10 k Pa, and the combined expanded uncertainties Uc (S) for each set of data was given in the table and Uc (log K_{SP}) ≤ 0.01. (Level of confidence = 0.95).

$$K_{SP} = \left[Th^{4+}\right][OH^{-}]^{4} \quad (3)$$

$$Where, \ \left[Th^{4+}\right] = Th_{Ionic} + Th_{Polymeric} \quad (4)$$

Table 4 presents the estimated solubility (S) and solubility products (as log K_{SP}) with the inclusion and exclusion of colloidal thorium as soluble thorium content. The solubility product values determined in the present studies are found to span over four orders of magnitude. The literature data on solubility product values have wide spread(log K_{SP} varies from −45.5 to −54.2). The nature of solubility limiting phase, experimental conditions, equilibration periods, methodologies to estimate the thorium content, and majorly the inclusion of colloids as soluble thorium content could explain these large discrepancies in the literature reported data (Mompean, 2007). The accountancy for colloids to estimate the solubility limits as shown in present studies could support the widely spread literature data on solubility products. Solubility (or log K_{SP}) decreases with both the ionic strength and initial equilibrated pH, whether the colloid formation is accounted or not to estimate the solubility (or log K_{SP}) values. The ionic strength and initial equilibrated pH of the sample plays a key role in solubility estimations. For a particular initial equilibrated pH, solubility (or log K_{SP}) decreases with ionic strength; while for a particular ionic strength, the same trend is observed with increase in initial equilibrated pH. The inclusion of colloid fraction in soluble content overestimates log K_{SP} values to almost 2–4 orders depending on the initial experimental conditions. The variations in the solubility products calculated in the present study and in the literature reported data can also be explained on the basis of the precipitation in the present work. This discrepancies can be explained on the basis of fraction of thorium present as amorphous $Th(OH)_4$ and as crystalline/microcrystalline ThO_2 in precipitate formed under the present experimental conditions. The higher ionic strength and higher pH would favor an early precipitate formation, that can stabilize more towards crystalline form (ThO_2) than the amorphous form ($Th(OH)_4$). This could be attributed to the observed trend of solubility (or log K_{SP}) values with increase in ionic strength (at identical initial pH) or pH (at identical ionic strength).

4. Conclusion

The release of thorium to aquatic environments from the waste or storage confinements is majorly determined by its solubility limits. Further, the different kind of thorium species such as ionic, polymeric, and colloidal forms behave differently in geochemical environments. The present studies provide detailed insights on role of intrinsic colloid particles on solubility (log K_{SP}) estimation. The LIBD was vitally employed to determine the size and concentration of the colloids of very small size (as low as 13 nm) and at very low concentrations (as low as 10^{10} particles/mL) in the supernatants of the long equilibrated (~3 years) samples. The chemical form of thorium is a key concern to decide the kind of interaction or physiochemical phenomenon; and its capability to migrate or retard in the geochemical environments. The present studies also fractionated different kind of soluble thorium content present in supernatants to ionic, polymeric, and colloidal thorium forms, both qualitatively and quantitatively. The precipitate formed was also characterized by XRD, and TG-DSC, which showed that the precipitate formed is neither completely $Th(OH)_4$ nor $ThO_2.2H_2O$; but intermediate between the two forms. The thorium content contributing to non-colloidal form only (ionic or polymeric species) was used to estimate the true solubility and solubility products of amorphous thorium hydroxide. The accountancy of colloids in solubility estimation showed discrepancies of 2–4 orders of magnitude to that of their exclusion to the same. Future directions revealing the role of inorganic, organic complexants and the effect of various environmental conditions could be carried as a step towards to match the naturally occurring geochemical environments.

Declaration of competing interest

The authors declare that they have no known competing financial interests or personal relationships that could have appeared to influence the work reported in this paper.

Appendix A. Supplementary data

Supplementary data to this article can be found online at https://doi.org/10.1016/j.chemosphere.2020.129327.

References

Allard, B., Olofsson, U., Torstenfelt, B., 1984. Environmental actinide chemistry. Inorg. Chim. Acta. 94, 205–221.
Altmaier, M., Neck, V., Müller, R., Fanghänel, Th, 2005. Solubility of ThO2·xH2O(am) in carbonate solution and the formation of ternary Th(IV) hydroxide-carbonate complexes. Radiochim. Acta 93, 83–92.
Bates, J.K., Bradley, J.P., Teetsov, A., Bradley, C.R., Brink, M.B., 1992. colloid formation during waste form reaction: implications for nuclear waste disposal. Science 256, 649–651.
Bitea, C., Müller, R., Neck, V., Walther, C., Kim, J.I., 2003. Study of the generation and stability of thorium(IV) colloids by LIBD combined with ultra filtration. Colloid. Surface. Physicochem. Eng. Aspect. 217, 63–70.
Bundschuh, T., Knopp, R., Müller, R., Kim, J.I., Neck, V., Fanghänel, Th, 2000. Application of LIBD to the determination of the solubility product of thorium(IV)-

colloids. Radiochim. Acta 88, 625–629.
Brown, M., BaohuaGu, 2006. In: Gu, B., Coates, J.D. (Eds.), Chapter 2: the Chemistry of Perchlorate in the Environment in Perchlorate: Environmental Occurrence, Interactions and Treatment. Springer.
Choppin, G.R., Jensen, M.P., 2010. In: Morss, Lester R., Edelstein, Norman M., Fuger, Jean (Eds.), Chapter Twenty Three: Actinides in Solution - Complexation and Kinetics in the Chemistry of the Actinide and Transactinide Elements, fourth ed. Springer, Dordrecht, The Netherlands.
Henry, M., Jolivet, J.P., Livage, J., 1992. Aqueous chemistry of metal cations: hydrolysis, condensation and complexation. In: Reisfeld, R., JJørgensen, C.K. (Eds.), Chemistry, Spectroscopy and Applications of Sol-Gel Glasses, vol. 77. Structure and Bonding, pp. 153–206.
Honeyman, B.D., 1999. Colloidal culprits in contamination. Nature 397, 23–24.
Jernstrom, J., Vuorinen, U., Hakanen, M., Niskanen, A., 2001. Solubility of thorium under anoxic conditions. Radiochemistry 43, 4653 470.
Johansson, G., 1968. On the structure of the hydrolysis products of thorium. Acta Chem. Scand. 22, 399–409.
Kalmykov, S.N., Denecke, M.A., 2011. Actinide Nanoparticle Research. Springer-Verlag Berlin Heidelberg.
Kim, J.I., Buckau, G., Klenze, R., 1987. Natural Colloids and Generation of Actinide Pseudocolloids in Groundwater. Springer Netherlands, pp. 289–299.
Kim, J.I., Walther, C., 2006. Laser-induced breakdown detection (chapter 12). In: Wilkinson, K.J., Lead, J.R. (Eds.), Environmental Colloids and Particles: Behaviour, Separation and Characterisation, vol. 10. John Wiley & Sons, Ltd, Chichester, UK.
Knope, K.E., Wilson, R.E., Vasiliu, M., Dixon, D.A., Soderholm, L., 2011. Thorium(IV) molecular clusters with a hexanuclear Th core. Inorg. Chem. 50, 9696–9704.
Knope, K.E., Soderholm, L., 2013. Solution and solid-state structural chemistry of actinide hydrates and their hydrolysis and condensation products. Chem. Rev. 113, 944–994.
Mompean, F.J. (Ed.), 2007. Chemical Thermodynamics of Thorium. OECD Nuclear Energy Agency, Data Bank Issy-les-Moulineaux, (France), 2007.
Natrajan, L.S., Swinburne, A.N., Andrews, M.B., Randall, S., Heath, S.L., 2014. Redox and environmentally relevant aspects of actinide(IV) coordination chemistry. Coord. Chem. Rev. 171–193, 266–267.
Neck, V., Kim, J.I., 2001. Solubility and hydrolysis of tetravalent actinides. Radiochim. Acta 89, 1–16.
Neck, V., Müller, R., Bouby, M., Altmaier, M., Rothe, J., Denecke, M.A., Kim, J.I., 2002. Solubility of amorphous Th(IV) hydroxide – application of LIBD to determine the solubility product and EXAFS for aqueous speciation. Radiochim. Acta 90, 485–494.
Neck, V., Altmaier, M., Müller, R., Bauer, A., Fanghänel, Th, Kim, J.I., 2003. Solubility of crystalline thorium dioxide. Radiochim. Acta 91, 253–262.
Rai, D., Moore, D.A., Oakes, C.S., Yui, M., 2000. Thermodynamic model for the solubility of thorium dioxide in the Na+-Cl−-OH−-H2O system at 23° C and 90° C. Radiochim. Acta 88, 297–306.
Rao, D.R.M., Rawat, N., Manna, D., Sawant, R.M., Ghanty, T.K., Tomar, B.S., 2013. Complexation of thorium with pyridine monocarboxylates: a thermodynamic study by experiment and theory. J. Chem. Thermodyn. 58, 432–439.
Rothe, J., Denecke, M.A., Neck, V., Muller, R., Kim, J.I., 2002. XAFS investigation of the structure of aqueous thorium(IV) species, colloids, and solid thorium(IV) oxide/hydroxide. Inorg. Chem. 41, 249–258.
Ryan, J.L., Rai, D., 1987. Thorium(IV) hydrous oxide solubility. Inorg. Chem. 26, 4140–4142.
Silva, R., Nitsche, H., 1995. Actinide environmental chemistry. Radiochim. Acta 70–71, 377–396.
Walther, C., 2003. Comparison of colloid investigations by single particle analytical techniques - a case study on thorium-oxyhydroxides. Colloid. Surface. Physicochem. Eng. Aspect. 217, 81–92.
Walther, C., Fuss, M., Büchner, S., 2008. Formation and hydrolysis of polynuclear Th(IV) complexes - a nano-electronspray mass-spectrometry study. Radiochim. Acta 96, 411–425.
Walther, C., Denecke, M.A., 2013. Actinide colloids and particles of environmental concern. Chem. Rev. 113, 995–1015.
Wickleder, M.S., Fourest, B., Dorhout, P.K., 2010. In: Morss, Lester R., Edelstein, Norman M., Fuger, Jean (Eds.), Chapter Three: Thorium in the Chemistry of the Actinide and Transactinide Elements, fourth ed. Springer, Dordrecht, The Netherlands, pp. 117–126.
Xia, Y., Felmy, A.R., Rao, R., Wang, Z., Hess, N.J., 2003. Thermodynamic model for the solubility of ThO2(am) in the aqueous Na+-H+-OH−-NO3−-H2O-EDTA system. Radiochim. Acta 91, 751–760.